Naval Research Laboratory
Washington, DC 20375-5320

NRL/MR/6930--17-9733

Bioinspired Surface Treatments for Improved Decontamination: Silicon and Latex Polymer SLIPS Treatments

Brandy J. White
Martin H. Moore

Laboratory for the Study of Molecular Interfacial Interactions
Center for Bio/Molecular Science & Engineering

Anthony P. Malanoski

Laboratory for Biosensor and Biomaterials
Center for Bio/Molecular Science & Engineering

Chanté Campbell

Howard University
Washington, DC

June 27, 2017

REPORT DOCUMENTATION PAGE

Form Approved
OMB No. 0704-0188

1. REPORT DATE *(DD-MM-YYYY)* 27-06-2017	**2. REPORT TYPE** NRL Memorandum Report	**3. DATES COVERED** *(From - To)* October 7, 2015 – January 30, 2017

4. TITLE AND SUBTITLE

Bioinspired Surface Treatments for Improved Decontamination: Silicon and Latex Polymer SLIPS Treatments

5a. CONTRACT NUMBER

5b. GRANT NUMBER

5c. PROGRAM ELEMENT NUMBER

6. AUTHOR(S)

Brandy J. White, Martin H. Moore, Anthony P. Malanoski, and Chanté Campbell*

5d. PROJECT NUMBER

5e. TASK NUMBER

5f. WORK UNIT NUMBER

69-1C75

7. PERFORMING ORGANIZATION NAME(S) AND ADDRESS(ES)

Naval Research Laboratory, Code 6930
4555 Overlook Avenue, SW
Washington, DC 20375-5320

8. PERFORMING ORGANIZATION REPORT NUMBER

NRL/MR/6930--17-9733

9. SPONSORING / MONITORING AGENCY NAME(S) AND ADDRESS(ES)

Defense Threat Reduction Agency
DTRA-Joint CBRN Center of Excellence
BLDG E-2800
APG-EA, MD 21010

10. SPONSOR / MONITOR'S ACRONYM(S)

DTRA–CB10125

11. SPONSOR / MONITOR'S REPORT NUMBER(S)

12. DISTRIBUTION / AVAILABILITY STATEMENT

Approved for public release; distribution is unlimited.

13. SUPPLEMENTARY NOTES

*NRL Summer Intern, Chemistry Department, Howard University, Washington, DC

14. ABSTRACT

This effort evaluates bioinspired coatings for use in a top-coat type application to identify those technologies that may improve decontamination capabilities for painted surfaces. This report details results for evaluation of variations on two slippery liquid-infused porous surfaces (SLIPS) produced by Pacific Northwest National Laboratory (PNNL; Richland, WA). Retention of the simulants paraoxon, methyl salicylate, dimethyl methylphosphate, and diisopropyl fluorophosphates following treatment of contaminated surfaces with a soapy water solution is reported. Wetting behaviors and target droplet diffusion on the surfaces are also discussed.

15. SUBJECT TERMS

Coatings
Paint
Decontamination

16. SECURITY CLASSIFICATION OF:			**17. LIMITATION OF ABSTRACT**	**18. NUMBER OF PAGES**	**19a. NAME OF RESPONSIBLE PERSON** Brandy J. White
a. REPORT Unclassified Unlimited	**b. ABSTRACT** Unclassified Unlimited	**c. THIS PAGE** Unclassified Unlimited	SAR	34	**19b. TELEPHONE NUMBER** *(include area code)* (202) 404-6100

CONTENTS

FIGURES

TABLES

EXECUTIVE SUMMARY

The Center for Bio/Molecular Science and Engineering at the Naval Research Laboratory (NRL) initiated a program in January 2015 for evaluation of bioinspired treatments suitable for use as a top coat on painted surfaces with the intention of achieving improved aqueous decontamination of these materials. Funding was provided by the Defense Threat Reduction Agency (DTRA, CB10125). This report details results for evaluation of variations on two slippery liquid-infused porous surfaces (SLIPS) produced by Pacific Northwest National Laboratory (PNNL; Richland, WA). The SLIPS surfaces use either a sprayable silicon base or a strippable latex base. Retention of the simulants paraoxon, methyl salicylate, dimethyl methylphosphate, and diisopropyl fluorophosphates following treatment of contaminated surfaces with a soapy water solution is reported. Wetting behaviors and target droplet diffusion on the surfaces are also discussed.

BIOINSPIRED SURFACE TREATMENTS FOR IMPROVED DECONTAMINATION: SILICON AND LATEX SLIPS TREATMENTS

INTRODUCTION

The DoD Chemical and Biological Defense Program (CBDP) seeks to provide protection of forces in a contaminated environment including contamination avoidance, individual protection, collective protection, and decontamination. In January 2015, the Center for Bio/Molecular Science and Engineering at the Naval Research Laboratory (NRL) began an effort funded through the Defense Threat Reduction Agency (DTRA, CB10125) with a view toward evaluation and development of top-coat type treatments suitable for application to painted surfaces that would reduce retention of chemical threat agents following standard decontamination approaches. The effort sought to survey relevant and related areas of research and evaluate identified technologies under appropriate methods to determine efficacy, scalability, and durability.

The current document summarizes results for one group of the identified technologies. Slippery liquid-infused porous surfaces (SLIPS) comprise a film of lubricating liquid with a textured substrate (micro/nano or both). [1, 2, 3, 4] This provides a surface that is effectively smooth on the molecular scale and a liquid-liquid interaction interface for contaminants. The liquid-liquid interface is in contrast to the commonly harnessed lotus leaf effect that is achieved through use of a textured surface providing air-liquid and air-solid interfaces. The polymer and liquid components of a SLIPS system are selected to repel liquids of interest.

The Pacific Northwest National Laboratory (PNNL) slippery liquid-infused porous surfaces were developed with a focus on prevention of biofouling; the conditions considered here are not directly in line with the original application. The formulations are based either on a sprayable silicon based polymer layer or a latex based polymer layer. The silicon polymer has been infused with either silicone oil (poly(dimethylsiloxane) (PDMS)-based; viscosity 10 cST, 25°C; PNNL1) or a fluorocarbon oil (Krytox 103; PNNL2). A polymer only variation was also provided (PNNL5). The latex based polymer system was provided with (PNNL3) and without (PNNL4) fluorocarbon oil (Krytox 103). Polymer only variants (PNNL4 and PNNL5) provide points of comparison for the SLIPS approach versus a more typical textured polymer approach.

Here, aluminum coupons painted with a polyurethane paint system were provided to scientists at PNNL. PNNL treated these coupons and returned them to NRL for evaluation (Figure 1). The coupons were subjected to the standard evaluations including measurement of sessile, sliding, and shedding contact angles, target spreading, and quantification of retention for the simulant compounds.

Manuscript approved May 25, 2017.

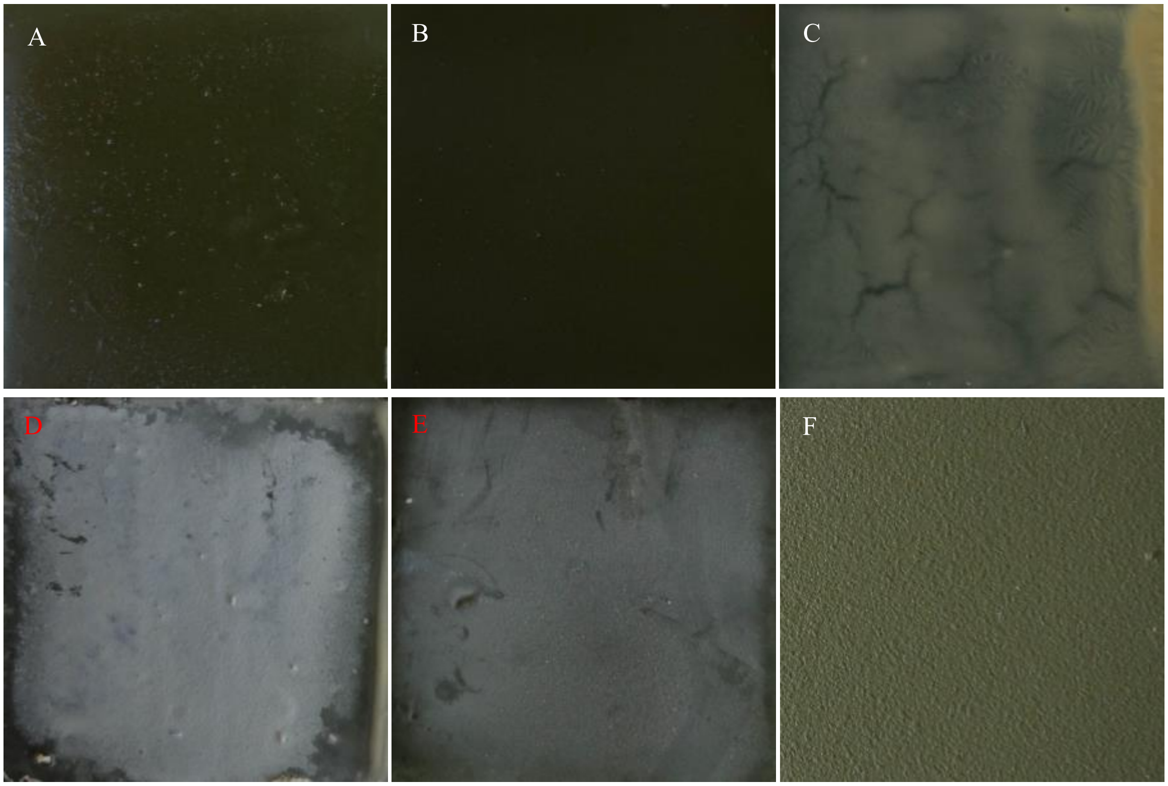

Fig. 1 — Images of the five types of PNNL samples: PNNL1, sprayable silicon polymer with silicone oil (A), sprayable silicon base with fluorocarbon oil (B), latex polymer with fluorocarbon oil (C), latex polymer only (D), and silicon polymer only (E). An image of a paint only coupon has been included for comparison (F).

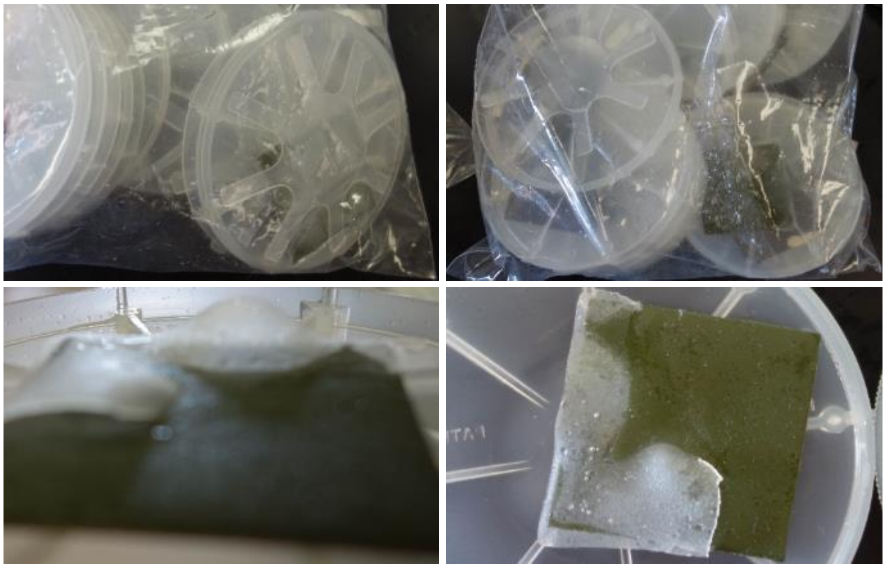

Fig. 2 — Images of PNNL samples collected during unpacking. Single coupon images (bottom) are of a PNNL1 sample.

METHODS

Sessile contact angles for samples evaluated under this effort used three 3 μL droplets per surface with each droplet measured independently three times for each of three targets, water, ethylene glycol, and n-heptane (average of 9 measurements for each liquid). Geometric surface energy was calculated based on the water and ethylene glycol interactions using software designed for the DROPimage goniometer package. Sliding angles were determined using 5 μL droplets. The droplet was applied at 0° after which the supporting platform angle was gradually increased up to 60°. Sliding angles for each of the liquids were identified as the angle for which movement of the droplet was identified. Shedding angles for each liquid were determined using 12 μL droplets initiated 2.5 cm above the coupon surface. Changes in base angle of 10° were utilized to identify the range of droplet shedding angle based on a complete lack of droplet retention by the surface (not sliding). The angle was then reduced in steps of 1° to identify the minimum required angle. In order to analyze agent spreading on the surfaces, droplets of 5 μL were applied to the surfaces and images were collected at 30 s intervals for 5 min followed by images at 5 min intervals for a total of 30 min. Droplet diameters were determined using tools provided by Adobe Photoshop CS3. DFP samples were kept covered for the duration of the experiment to minimize evaporation. In some cases, reflections from the glass cover can be seen in those images.

Simulant exposure and evaluation methods were based on the tests developed by Edgewood Chemical Biological Center referred to as Chemical Agent Resistance Method (CARM). [5] Standard target exposures utilized a challenge level of 10 g/m^2. The coupons provided by PNNL were 0.002581 m^2; the 10 g/m^2 target challenge was applied to the surfaces as four neat droplets. Following application of the target, coupons were aged 1 h. A gentle stream of air is then used to expel target from the surface prior to rinsing with soapy water (0.59 g/L Alconox in deionized water). Finally, the coupons were soaked in isopropanol for 30 min to extract any remaining target; this isopropanol extract was analyzed by the appropriate chromatography method to determine target retention on the surface.

For paraoxon analysis, a Shimadzu High Performance Liquid Chromatography (HPLC) system with dual-plunger parallel flow solvent delivery modules (LC-20AD) and an auto-sampler (SIL-20AC; 40 μL injection volume) coupled to a photodiode array detector (SPD-M20A; 277 nm) was used. The stationary phase was a C18 stainless steel analytical column (Luna, 150 mm x 4.6 mm, 3 μm diameter; Phenomenex, Torrance, CA) with an isocratic 45:55 acetonitrile: 1% aqueous acetic acid mobile phase (1.2 mL/min). [6] For analysis of methyl salicylate (MES), diisopropyl fluorophosphates (DFP), and dimethyl methylphosphonate (DMMP), gas chromatography-mass spectrometry (GC-MS) was accomplished using a Shimadzu GCMS-QP2010 with AOC-20 auto-injector equipped with a Restex RTX-5 (30 m x 0.25 mm ID x 0.25 μm df) cross bond 5% diphenyl 95% dimethyl polysiloxane column. A GC injection temperature of 200°C was used with a 1:1 split ratio at a flow rate of 3.6 mL/min at 69.4 kPa. The oven gradient ramped from 50°C (1 min hold time) to 180°C at 15°C/min and then to 300°C at 20°C/min where it was held for 5 min.

RESULTS

Upon receipt of the samples from PNNL, it was noticed that some damage had occurred during shipment. Several of the fluoroware containers were not sealed, allowing the samples to move within the plastic bags used as secondary packaging (Figure 2). It was also noted that some of the treatments were delaminating from the supporting painted coupon. Comments from PNNL indicate that delamination can occur for the coatings when excessive amounts of lubricant are loaded into the surface. Samples with obvious signs of delamination were not used for the described evaluations.

Analysis of the painted surfaces alone provides a point of comparison for evaluating the benefits of the surface treatments. Table 1 provides contact angles collected for coupons coated with the polyurethane paint system only. Table 1 also provides data collected for painted coupons that were oiled with the PDMS-based oil (viscosity 10 cST, 25°C;) prior to analysis.

As shown, all of the SLIPS treatments significantly increased the wetting angles for both water and ethylene glycol (PNNL1, 2, and 3; Table 1) over that of the painted surface alone. With the exception of the latex polymer only (no lubricant; PNNL4), samples did not achieve superhydrophobic water contact angles (>150°). Heptane wetted all surfaces, producing contact angles below the measurable threshold. Geometric surface energy was reduced by the SLIPS coatings as well as the polymer only treatments.

For the silicon polymer formulation, polymer with no lubricant (PNNL5) provided higher water and ethylene glycol contact angles and lower geometric surface energy than the lubricated versions (PNNL1 & 2). The polymer only version also yielded lower sliding and shedding angles for both water and ethylene glycol. The silicone oil infused silicon treatment (PNNL1) produced the lowest sessile and highest shedding angles of the three with sliding angles greater than 60°. In fact, simply oiling the painted surface resulted in a similar increase in water contact angle. Oiling the painted surface also resulted in similar shedding angles. The sample lubricated with fluorinated oil (PNNL2) provided distinctly improved shedding angles over that of the silicone oil sample (PNNL1).

For the latex polymer treatments, ethylene glycol contact angles were higher in the fluorocarbon lubricated samples (PNNL3) compared to the unlubricated polymer (PNNL4); however, water contact angles were higher for the polymer only samples. The water shedding angle for the polymer only sample is low (<10°), but inhomogenetity was observed across the surfaces. Depending on the sample, a greater or lesser degree of droplet pinning was observed. This is reflected by the lack of sliding on the surface. Shedding from the lubricated latex surfaces was observed at less than 25° for both water and ethylene glycol.

Table 1 – Sessile, Sliding, and Shedding Contact Angles

Coupon	**Liquid**	**Sessile Angle**	**Sliding Angle**	**Shedding Angle**	**Geometric Surface Energy (mJ/m^2)**
Paint Only					
Paint Only	water	47.5 ± 1.1	>60	>60	71.9 ± 5.1
	ethylene glycol	55.7 ± 2.1	>60	>60	
	n-heptane	--	--	--	
Oiled Paint	water	73.1 ± 2.1	>60	46.7 ± 3.3	32.2 ± 1.6
	ethylene glycol	52.5 ± 0.61	>60	49.8 ± 4.9	
	n-heptane	40.1 ± 2.9	>60	36.6 ± 3.3	
Silicon Polymer					
PNNL1	water	85.5 ± 2.2	>60	49 ± 3.0	21.2 ± 1.6
	ethylene glycol	74.5 ± 0.85	>60	47 ± 3.0	
	n-heptane	--	--	--	
PNNL2	water	111.1 ± 1.9	41.2 ± 8.0	25.0 ± 3.0	23.1 ± 2.4
	ethylene glycol	87.3 ± 1.1	44.7 ± 9.0	31.5 ± 5.0	

	n-heptane	--	--	--	
PNNL5	water	129.4 ± 1.2	6.75 ± 3.0	1.0 ± 3.0	13.3 ± 1.5
	ethylene glycol	110.4 ± 1.6	21.8 ± 3.0	13.4 ± 3.0	
	n-heptane	--	--	--	
Latex Polymer					
PNNL3	water	107.1 ± 0.67	25.7 ± 6.0	11.8 ± 5.0	13.0 ± 0.7
	ethylene glycol	95.7 ± 0.55	9.3 ± 2.5	21.4 ± 7.0	
	n-heptane	--	--	--	
PNNL4	water	152.6 ± 0.58	>60	9.3 ± 3.0	60.2 ± 8.5
	ethylene glycol	58.3 ± 3.73	>60	>60	
	n-heptane	--	--	--	

The tendency of droplets to spread across the surfaces was also evaluated. For these studies, 5 µL droplets of the simulants were utilized. The spread of the droplets was quantified by measuring the diameter of the droplets in the images over time (Figure 3). A full series of images is provided in the Appendix for each surface / target combination. For the paint only samples, DFP spreads quickly while MES slowly spreads across the surface; DMMP does not spread during the course of the 30 min incubation. When lubricated with the fluorocarbon oil (PNNL3), the silicon polymer based treatment reduces the spread of DFP as compared to the painted surface. The spread of MES is also reduced, while DMMP does not spread on this surface. Similarly, DMMP did not spread and MES spreading was minimal on the silicone oil lubricated variant (PNNL1). Interestingly, the spread of DFP was faster and to a greater extent on the silicone oil lubricated coupon than it was on the unlubricated coupon (PNNL5). The unlubricated version (PNNL5) significantly increased MES spreading. DMMP spreading was increased for both the lubricated (PNNL3) and unlubricated (PNNL4) versions of the latex polymer treatment. MES spreading was slightly reduced for these materials.

The coupons were subjected to several cycles of simulant exposure, aging, washing, and drying over a period of four weeks. The data reported here is for the initial round of exposures only. Extraction of the lubricated materials with isopropanol resulted in extraction of the lubricating oil as well as the deposited target. Again, result for the painted surface alone and for an oiled painted surface are included. Additional results are included for painted coupons that were not rinsed prior to isopropanol extraction, providing a point of reference for the total possible recovery of target. Though the nominal target application was 10 g/m^2, recovery from surfaces was always less than this value. Losses due to evaporation would be expected, especially for DFP. Additional losses likely occur during the rinse steps due to agent interaction with the untreated region of the coupon; the back of the coupons was untreated aluminum.

In the first round of exposures, retention of paraoxon, DMMP, and MES was significantly reduced by the lubricated SLIPS treatments (Figures 4 and 5; Table 2). Retention of DFP was increased for all SLIPS treatments. The silicon polymer only (PNNL5) treatment retained significant amounts of paraoxon, MES, and DFP (Figure 3); retained DMMP was 0.42 g/m^2. Lubrication of this surface with the silicone oil reduced retention of paraoxon and MES by 83 and 50%, respectively, as compared to the unlubricated variant. The use of fluorocarbon oil produced further reduction in paraoxon retention (94%) with some reduction of DFP retention (12%). DFP retention was significantly higher for the silicon polymer treatments (4.98 to 5.63 g/m^2) than for the paint only surface (0.52 g/m^2). Target retention by the latex polymer only treatment (PNNL4) was similar to that of the silicon polymer only (PNNL5) with the exception of a 72% reduction in paraoxon retention (Table 2). Lubrication of this treatment with fluorocarbon oil produced an order of magnitude reduction in paraoxon retention (2.39 g/m^2 to 0.29 g/m^2). DFP retention was increased upon lubrication; MES retention was decreased by 24%.

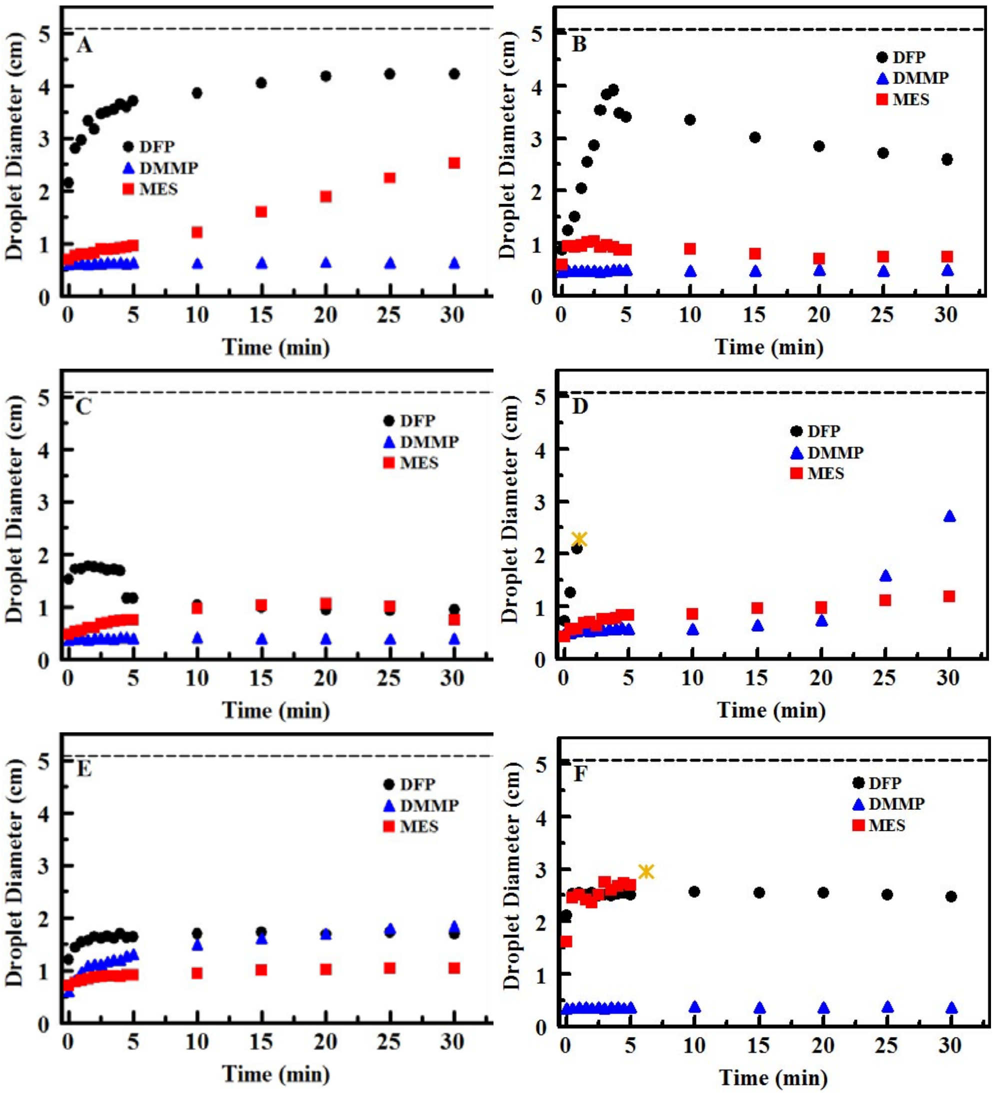

Fig. 3 — Progression of droplet diameters during incubation on the surfaces for DFP (black), DMMP (blue), and MES (red): painted coupon (A), PNNL1 (B), PNNL2 (C), PNNL3 (D), PNNL4 (E), PNNL5 (F). * Indicates the droplet is no longer visible on the surfaces (Panels D and F).

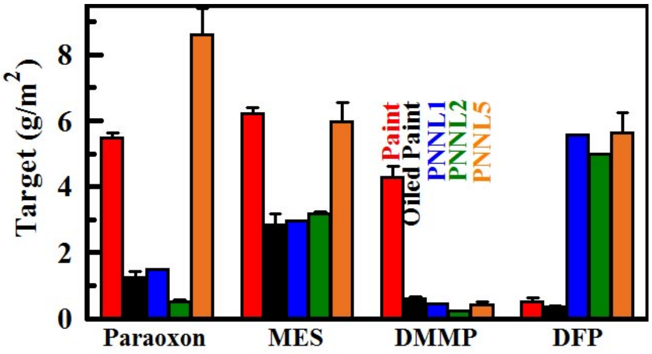

Fig. 4 — Target retention by coupons treated with silicon polymer variants following treatment with an air stream and rinsing with soapy water. Results for the paint only coupon included for comparison.

Table 2 – Target Retention (g/m^2) Following 1 h Aging

Coupon	**Description**	**Target**	**No Rinse**	**Air & Soapy Water**
Paint Only	Polyurethane paint system	paraoxon	9.84	5.48
		MES	9.54	6.20
		DMMP	9.90	4.28
		DFP	7.39	0.52
Oiled Paint	Polyurethane paint system with silicone oil	paraoxon		1.24
		MES		2.85
		DMMP		0.59
		DFP		0.34
PNNL1	Sprayable silicon based polymer with silicone oil	paraoxon		1.48
		MES		2.96
		DMMP		0.44
		DFP		5.55
PNNL2	Sprayable silicon based polymer with fluorocarbon oil	paraoxon		0.51
		MES		3.18
		DMMP		0.24
		DFP		4.98
PNNL3	Latex polymer with fluorocarbon oil	paraoxon		0.29
		MES		4.38
		DMMP		0.15
		DFP		3.90
PNNL4	Latex polymer with no lubricant	paraoxon		2.39
		MES		5.80
		DMMP		0.06
		DFP		2.87
PNNL5	Sprayable silicon based polymer with no lubricant	paraoxon		8.61
		MES		5.96
		DMMP		0.42
		DFP		5.63

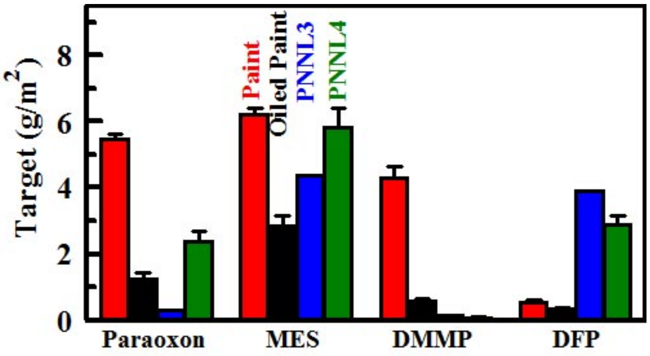

Fig. 5 — Target retention by coupons treated with latex polymer variants following treatment with an air stream and rinsing with soapy water. Results for the paint only coupon included for comparison.

In previous work with other SLIPS treatments, the increase in DFP retention was thought to be due to partitioning of the fluorinated target into the oil. With this interaction, the evaporation of the target would be reduced, and the target would not be available for removal during the rinse steps. Though the oiled, painted coupon retained less DFP than the paint only coupon, the potential for partitioning is not excluded. The oiled, painted coupon does not retain the oil following rinsing; it becomes part of the rinsate. The SLIPS treatments, however, retain the oil through the rinsing steps. It is removed during the isopropanol extraction. In other words, it is removed into the fraction that is analyzed for target content. The significant retention by polymer only treatments, however, would tend to exclude, or at least minimize, this partitioning as the retention mechanism for the PNNL samples.

Imaging studies for these materials noted something not previously observed. Typically (see appendix Figures A16 – A18), target droplets sit on the coating and slowly spread across the surface (as in DFP, Figure 3, Panel A). The appearance is of a gradually (or occasionally, rapidly) spreading puddle. Here, droplets appeared to be following this behavior and suddenly diverged; they appeared to be stable and diameters began to strongly change (Figure 3, Panels B, C, D) or droplets suddenly became visibly indistinguishable from the coating (Figure 3, Panels D and F). Appendix A, Figures A8, A9, and A13 provide good examples of the later. The slight color of the target can provide additional visualization in some cases. It appears, from these images, that the target is moving under the surface treatment rather than across the top of the material. Based on the lack of uniformity in the surfaces (Appendix) and the noted delamination of some samples, it is possible that breaks in the treatment provide access to the surface. Aqueous solutions (soapy water) would not be expected to penetrate to this part of the coating during rinse.

CONCLUSIONS

Delamination of the samples during shipping presents a concern and would necessitate modification of the formulations for improved durability. The samples analyzed for this report also failed to yield significant improvements over paint only surfaces. While the samples have low surface energy and moderate sliding / shedding behaviors, these characteristics are not correlated to low simulant retention. The likely partitioning of targets into the lubricating oil or through the polymer surface identifies a potential shortfall in this type of technology. Some of this additional target retention could potentially be eliminated or reduced by better adhesion to the surface and/or improved uniformity. While SLILPS treatments yield promising results in anti-graffiti and anti-icing studies, [3, 4] producing a single combination of polymer and lubricant that will not interact with the range of compounds considered to be chemical threat agents will prove challenging. Fluorinated compounds similar in structure to DFP, such as sarin, would be expected to partition into a fluorocarbon oil in a similar manner to that noted here. The fluorocarbon oil significantly reduced retention of paraoxon while slightly increasing retention of MES over that of the silicone oil. This type of retention might be controlled better through the use of a different polymer support material, for example a fluorinated polymer.

Given the physical characteristics of the specific materials considered here (thickness, opacity), lack of durability, and poor retention behavior, the PNNL treatments are unlikely to meet the needs of this effort. An alternative implementation might be possible in which the polymer / oil system is designed to prevent development of a secondary exposure hazard. In this case, the system would be designed to be strippable, retaining the target until the decontamination process, stripping, could be completed. In the meantime, the system would prevent exposure of personnel in the vicinity of the contaminated surface.

ACKNOWLEDGEMENTS

The samples, comments, and input provided by Dr. Curtis Larimer (PNNL) are appreciated. This research was sponsored by the Defense Threat Reduction Agency (DTRA, CB10125).

REFERENCES

1. I. Okada; S. Shiratori, "High-Transparency, Self-Standable Gel-SLIPS Fabricated by a Facile Nanoscale Phase Separation," *ACS Applied Materials & Interfaces* **6**, 1502-1508 (2014).
2. M.A. Samaha; M. Gad-el-Hak, "Polymeric Slippery Coatings: Nature and Applications," *Polymers* **6**, 1266-1311 (2014).
3. T.S. Wong; S.H. Kang; S.K.Y. Tang; E.J. Smythe; B.D. Hatton; A. Grinthal; J. Aizenberg, "Bioinspired self-repairing slippery surfaces with pressure-stable omniphobicity," *Nature* **477**, 443-447 (2011).
4. L.L. Xiao; J.S. Li; S. Mieszkin; A. Di Fino; A.S. Clare; M.E. Callow; J.A. Callow; M. Grunze; A. Rosenhahn; P.A. Levkin, "Slippery Liquid-Infused Porous Surfaces Showing Marine Antibiofouling Properties," *ACS Applied Materials & Interfaces* **5**, 10074-10080 (2013).
5. T. Lalain; B. Mantooth; M. Shue; S. Pusey; D. Wylie , "Chemical Contaminant and Decontaminant Test Methodology Source Document," US Army REDEC, Edgewood Chemical Biological Center,: Aberdeen Proving Ground, MD, ECBC-TR-980, 2nd Edition (2012).
6. Y.T. Gebreegzi; G.D. Foster; S.U. Khan, "Simulltaneous Determination of Carbaryl, Malathion, Fenitrothion, and Diazinon Residues in Sesame Seeds (*Seasmum indicum* L) " *J. Agric. Food Chem.* **48**, 5165-5168 (2000).

Appendix

COUPON IMAGES

Fig. A1 — DFP on a PNNL1 coupon. Images of a coupon before application (A) and at 0 (B), 0.5 (C), 1 (D), 1.5 (E), 2 (F), 2.5 (G), 3 (H), 3.5 (I), 4 (J), 4.5 (K), 5 (L), 10 (M), 15 (N), 20 (O), 25 (P), and 30 (Q) min following application of the target.

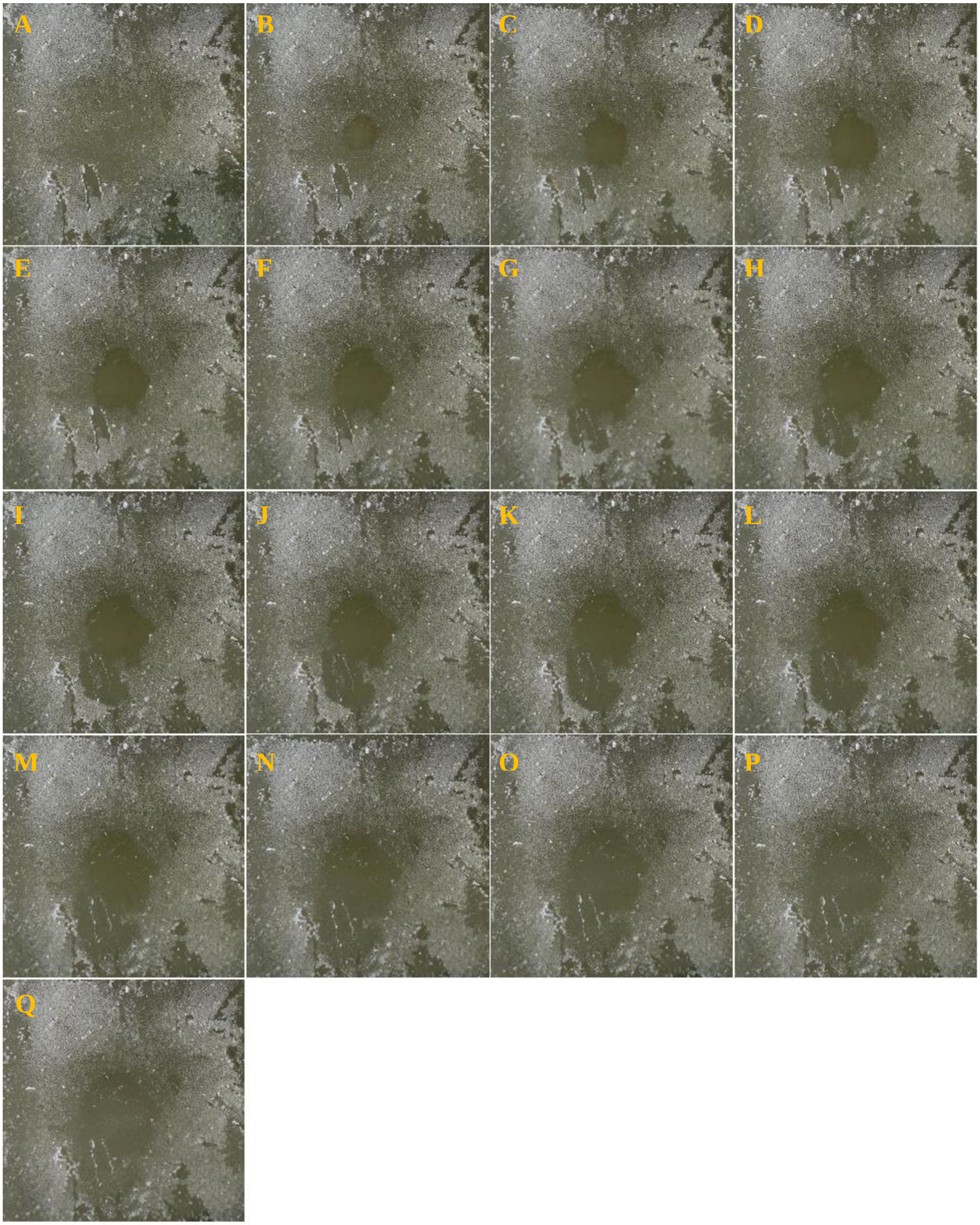

Fig. A2 — MES on a PNNL1 coupon. Images of a coupon before application (A) and at 0 (B), 0.5 (C), 1 (D), 1.5 (E), 2 (F), 2.5 (G), 3 (H), 3.5 (I), 4 (J), 4.5 (K), 5 (L), 10 (M), 15 (N), 20 (O), 25 (P), and 30 (Q) min following application of the target.

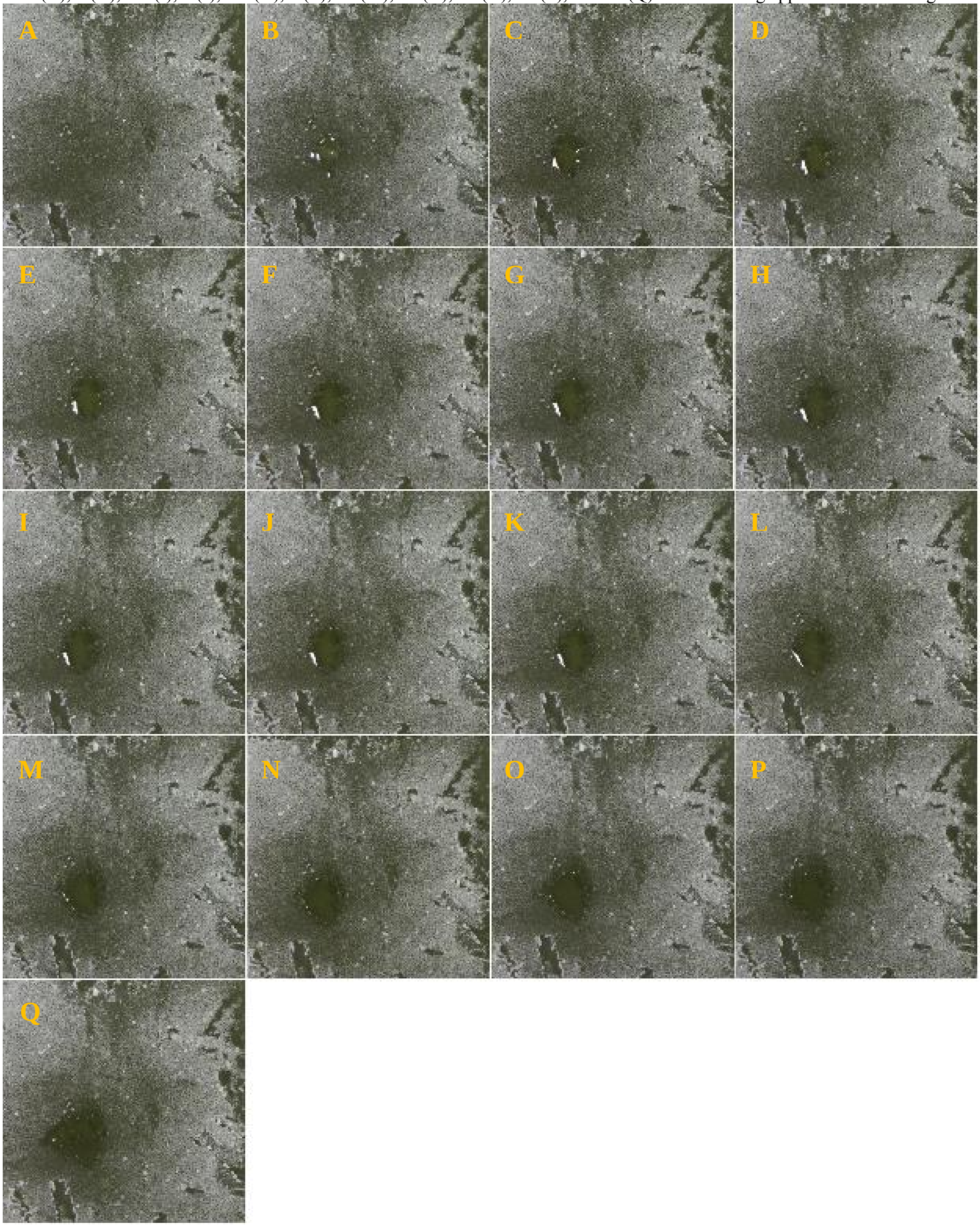

Fig. A3 — DMMP on a PNNL1 coupon. Images of a coupon before application (A) and at 0 (B), 0.5 (C), 1 (D), 1.5 (E), 2 (F), 2.5 (G), 3 (H), 3.5 (I), 4 (J), 4.5 (K), 5 (L), 10 (M), 15 (N), 20 (O), 25 (P), and 30 (Q) min following application of the target.

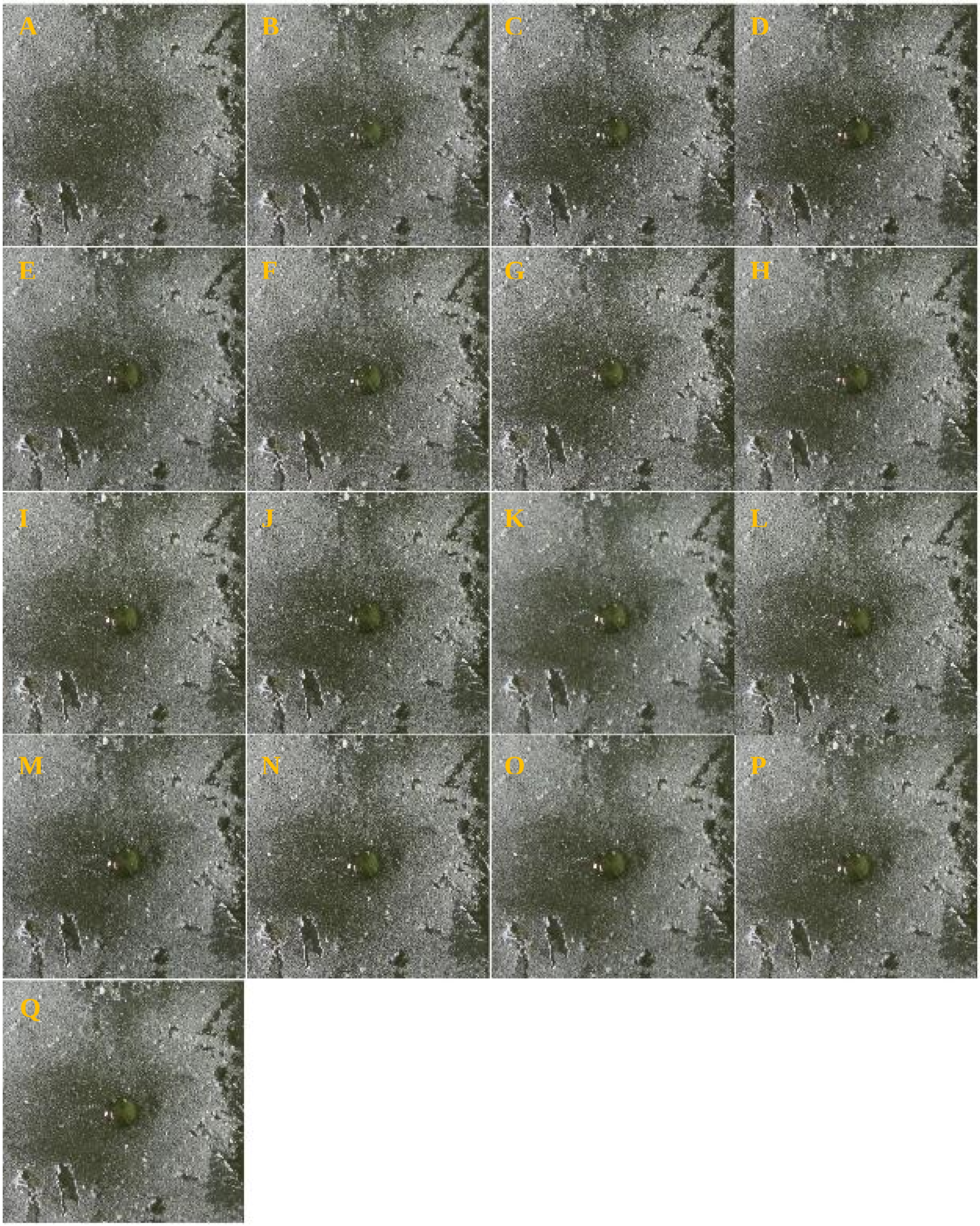

Fig. A4 — DFP on a PNNL2 coupon. Images of a coupon before application (A) and at 0 (B), 0.5 (C), 1 (D), 1.5 (E), 2 (F), 2.5 (G), 3 (H), 3.5 (I), 4 (J), 4.5 (K), 5 (L), 10 (M), 15 (N), 20 (O), 25 (P), and 30 (Q) min following application of the target.

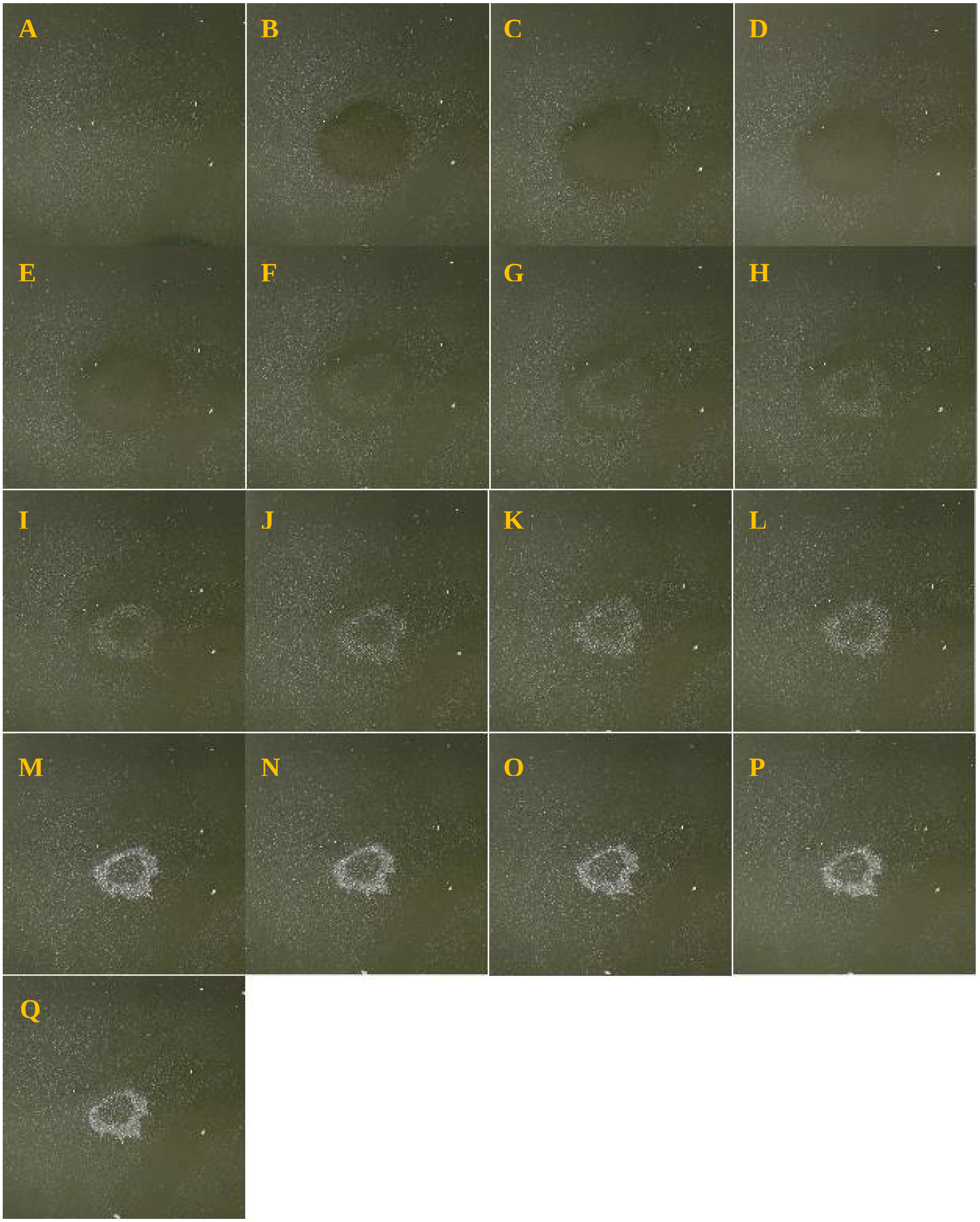

Fig. A5 — MES on a PNNL2 coupon. Images of a coupon before application (A) and at 0 (B), 0.5 (C), 1 (D), 1.5 (E), 2 (F), 2.5 (G), 3 (H), 3.5 (I), 4 (J), 4.5 (K), 5 (L), 10 (M), 15 (N), 20 (O), 25 (P), and 30 (Q) min following application of the target.

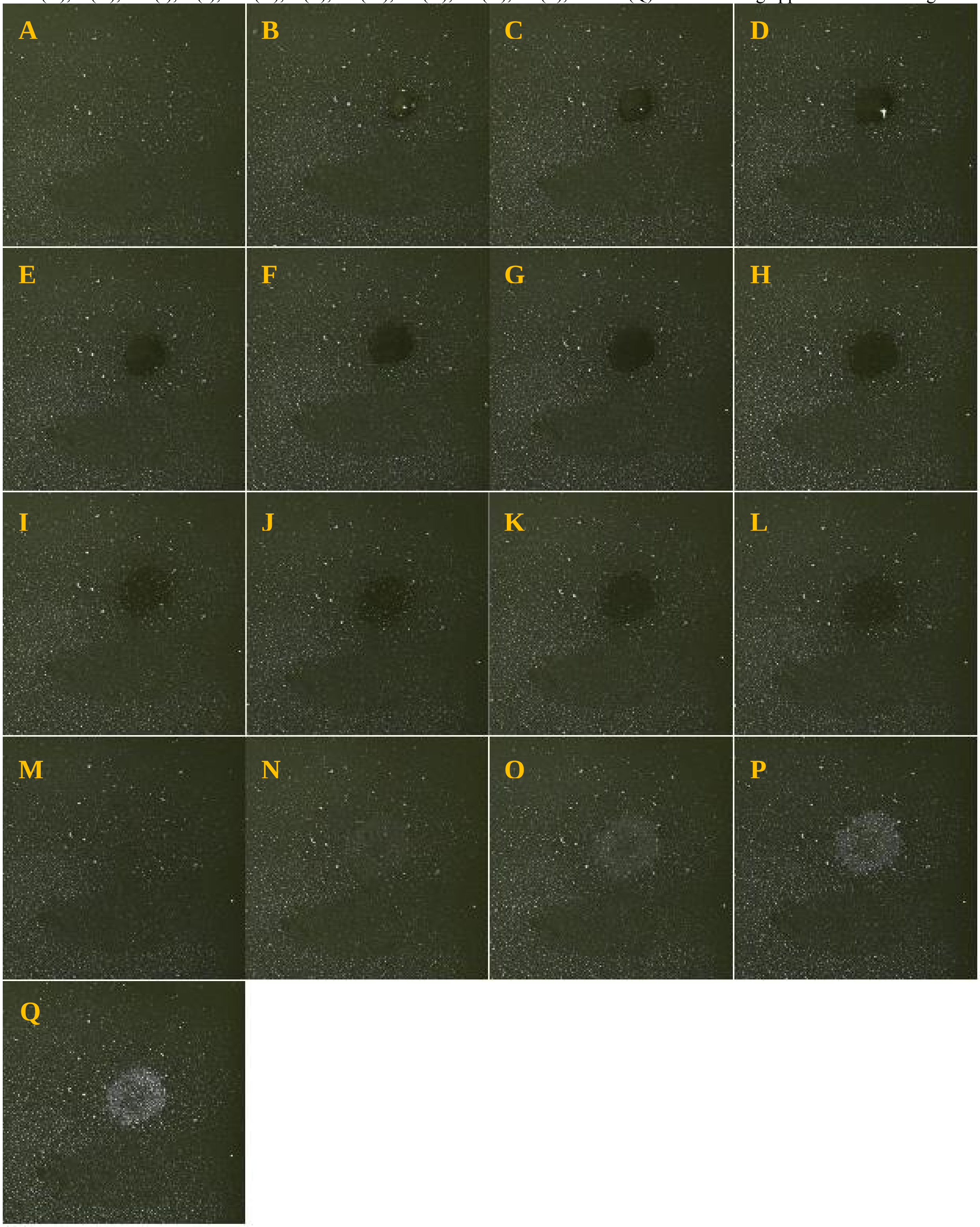

Fig. A6 — DMMP on a PNNL2 coupon. Images of a coupon before application (A) and at 0 (B), 0.5 (C), 1 (D), 1.5 (E), 2 (F), 2.5 (G), 3 (H), 3.5 (I), 4 (J), 4.5 (K), 5 (L), 10 (M), 15 (N), 20 (O), 25 (P), and 30 (Q) min following application of the target.

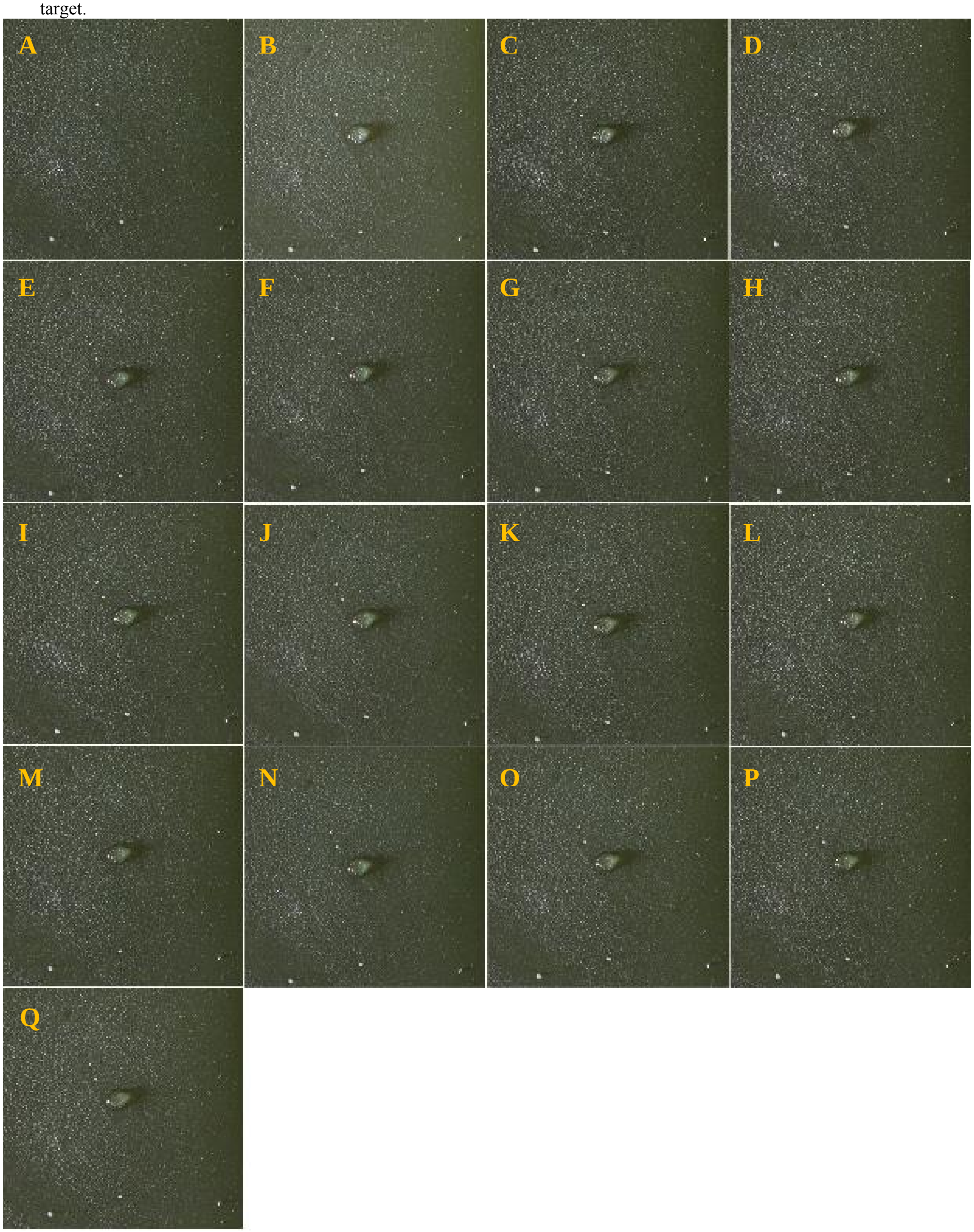

Fig. A7 — DFP on a PNNL3 coupon. Images of a coupon before application (A) and at 0 (B), 0.5 (C), 1 (D), 1.5 (E), 2 (F), 2.5 (G), 3 (H), 3.5 (I), 4 (J), 4.5 (K), 5 (L), 10 (M), 15 (N), 20 (O), 25 (P), and 30 (Q) min following application of the target.

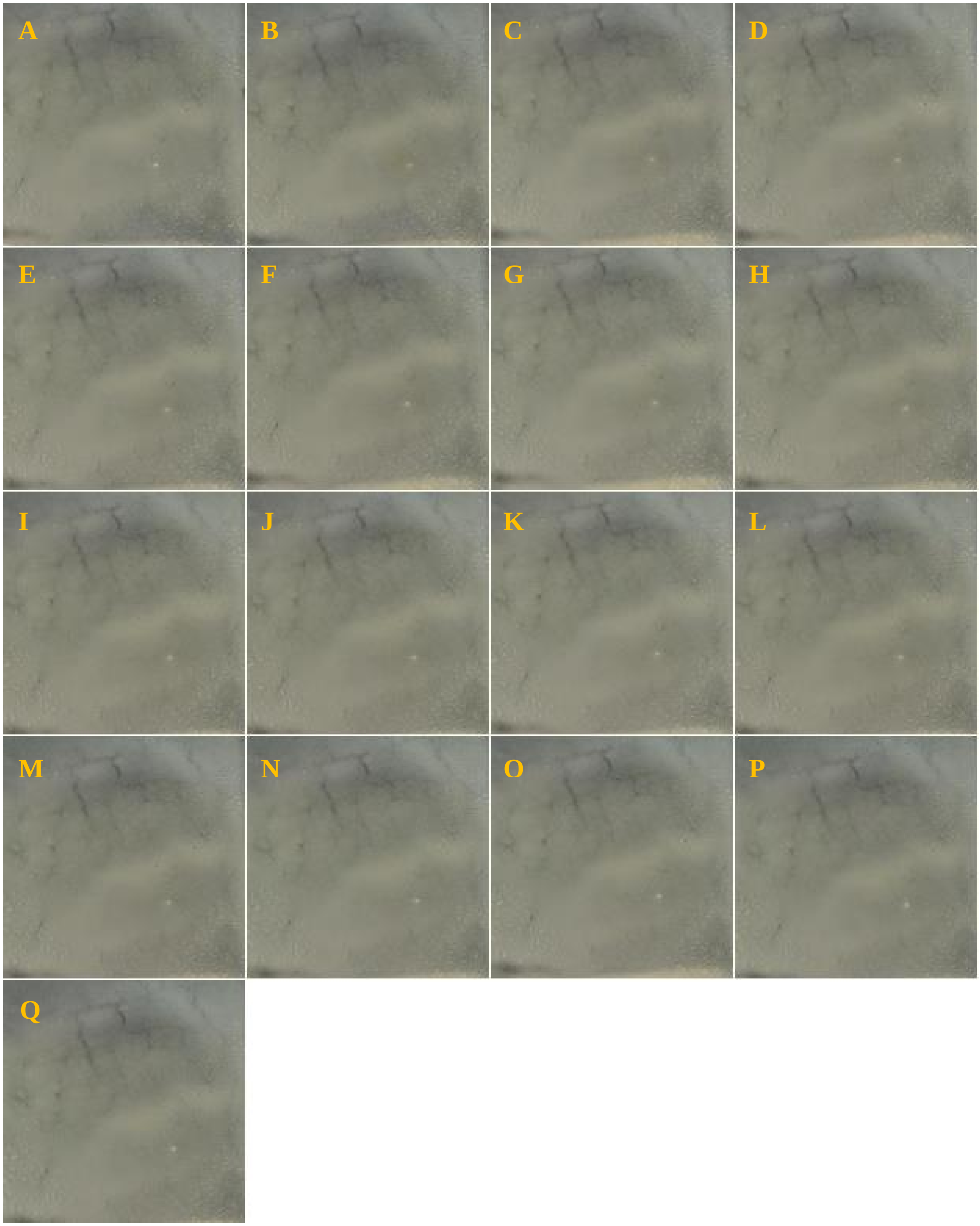

Fig. A8 — MES on a PNNL3 coupon. Images of a coupon before application (A) and at 0 (B), 0.5 (C), 1 (D), 1.5 (E), 2 (F), 2.5 (G), 3 (H), 3.5 (I), 4 (J), 4.5 (K), 5 (L), 10 (M), 15 (N), 20 (O), 25 (P), and 30 (Q) min following application of the target.

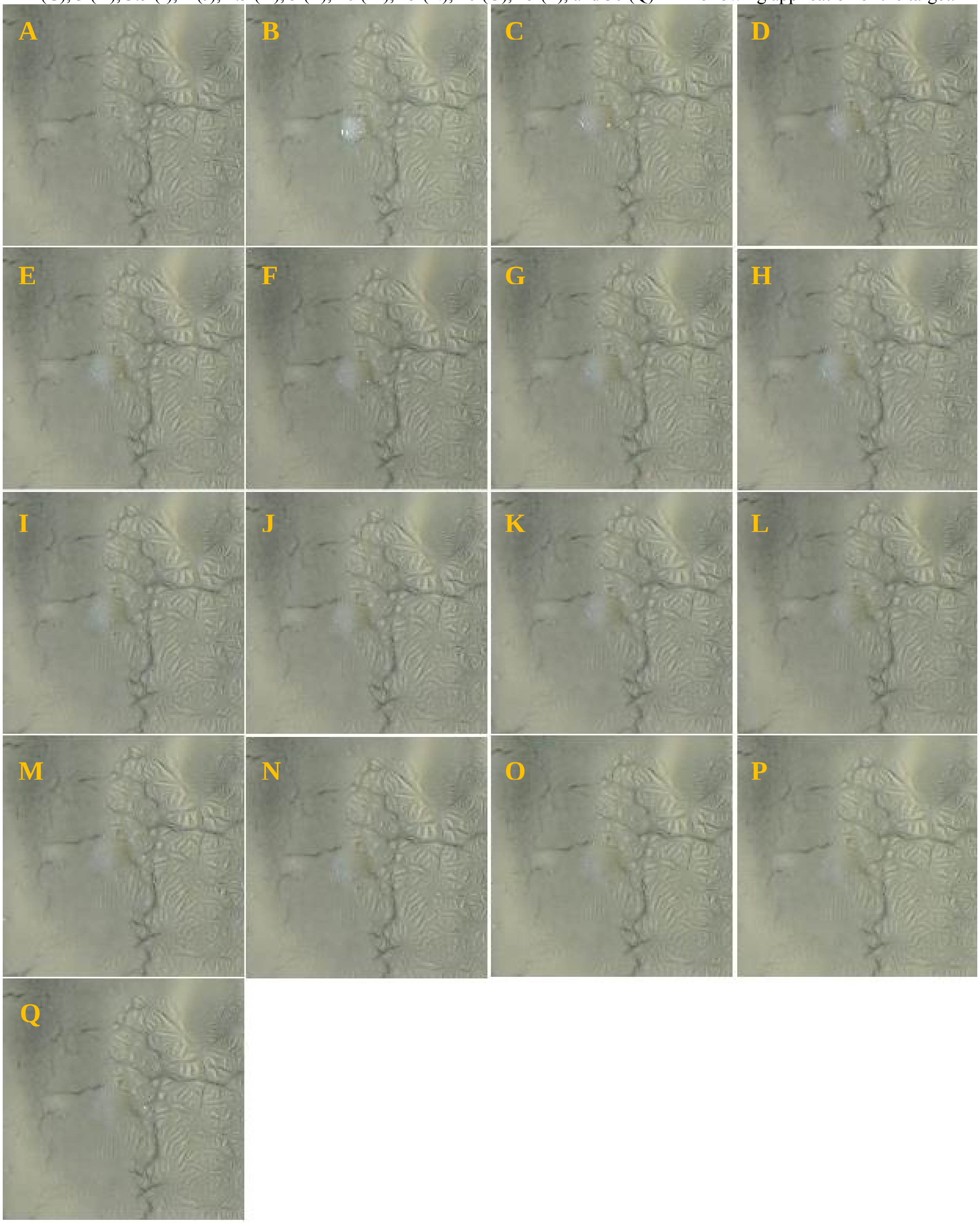

Fig. A9 — DMMP on a PNNL3 coupon. Images of a coupon before application (A) and at 0 (B), 0.5 (C), 1 (D), 1.5 (E), 2 (F), 2.5 (G), 3 (H), 3.5 (I), 4 (J), 4.5 (K), 5 (L), 10 (M), 15 (N), 20 (O), 25 (P), and 30 (Q) min following application of the target.

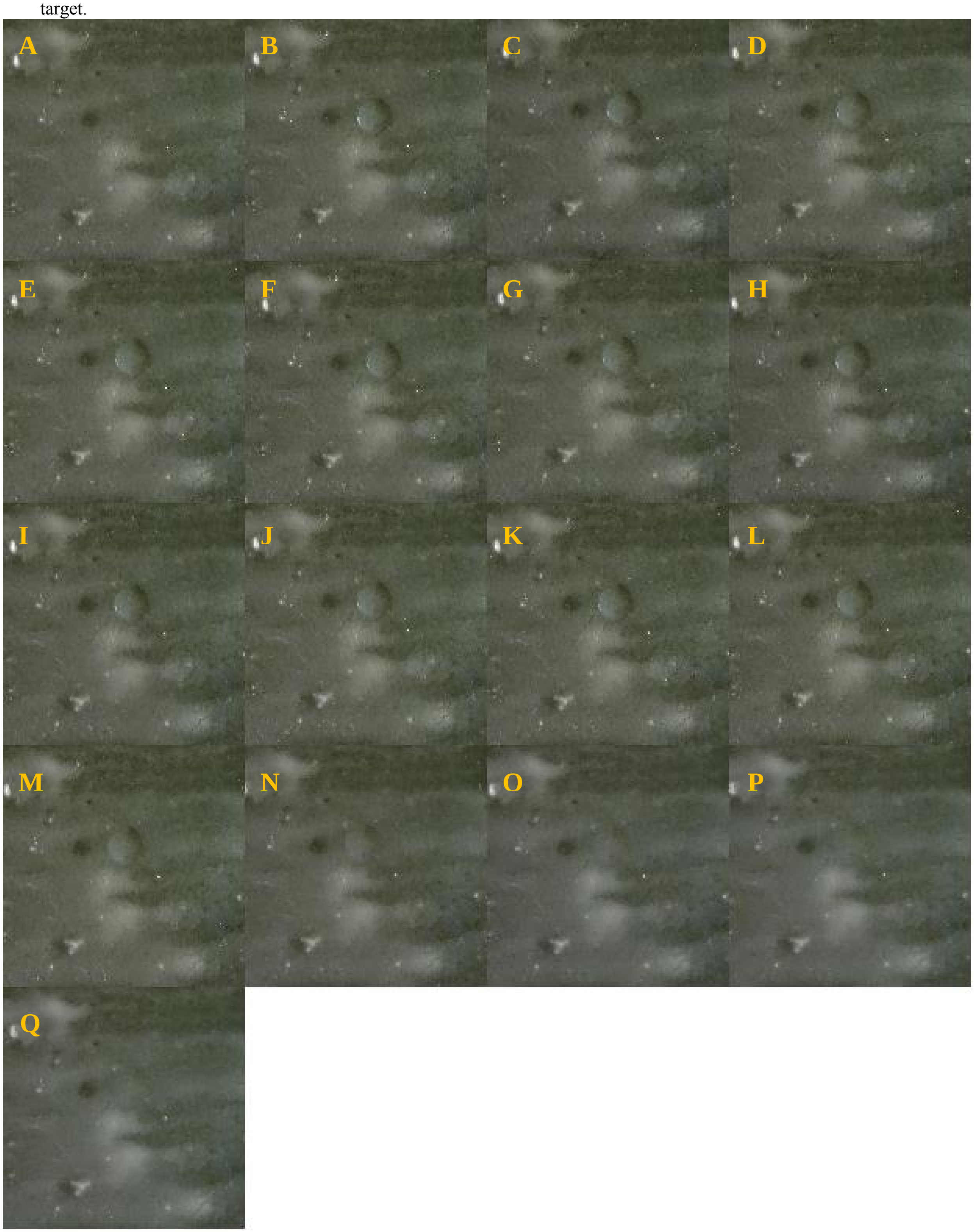

Fig. A10 — DFP on a PNNL4 coupon. Images of a coupon before application (A) and at 0 (B), 0.5 (C), 1 (D), 1.5 (E), 2 (F), 2.5 (G), 3 (H), 3.5 (I), 4 (J), 4.5 (K), 5 (L), 10 (M), 15 (N), 20 (O), 25 (P), and 30 (Q) min following application of the target.

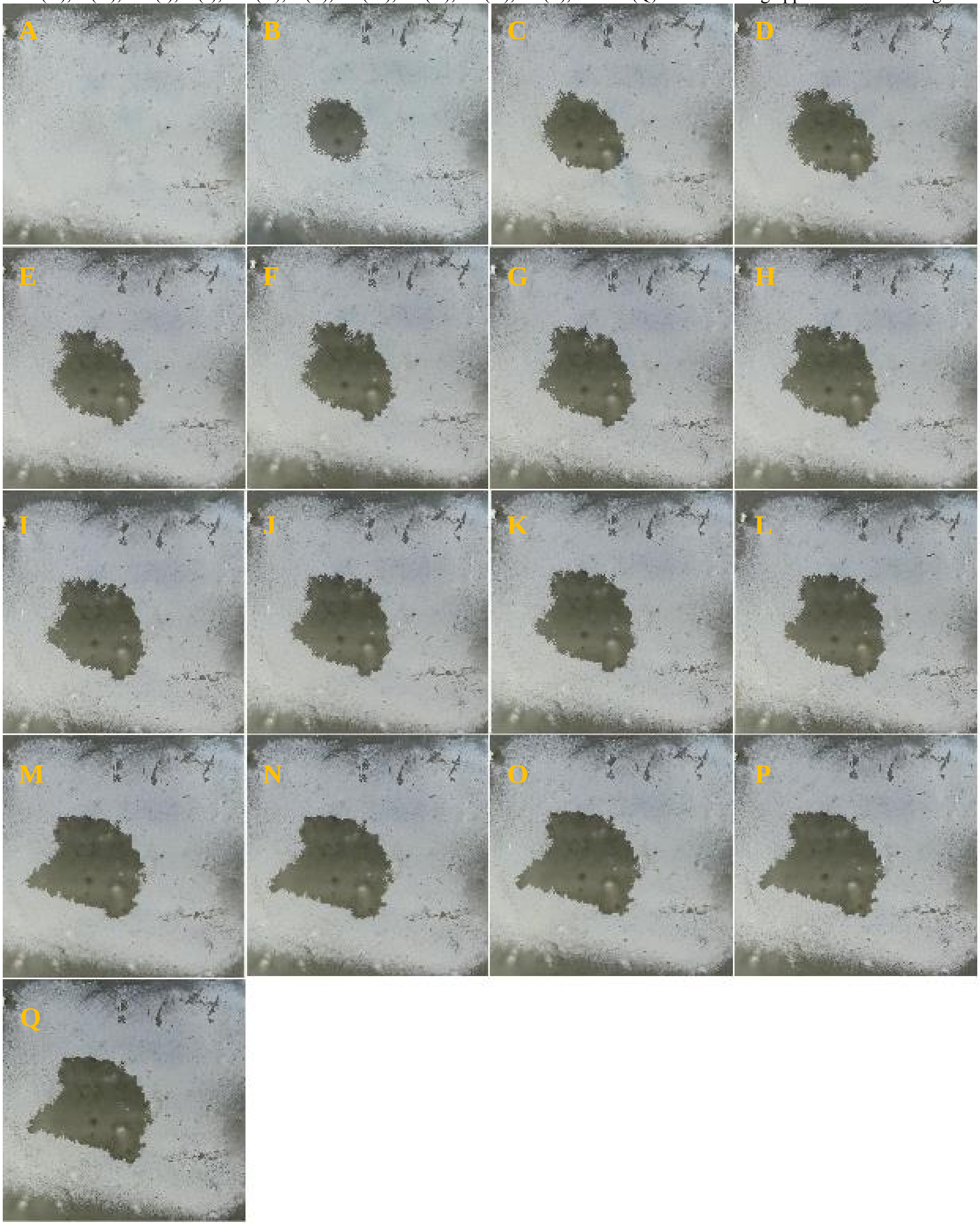

Fig. A11 — MES on a PNNL4 coupon. Images of a coupon before application (A) and at 0 (B), 0.5 (C), 1 (D), 1.5 (E), 2 (F), 2.5 (G), 3 (H), 3.5 (I), 4 (J), 4.5 (K), 5 (L), 10 (M), 15 (N), 20 (O), 25 (P), and 30 (Q) min following application of the target.

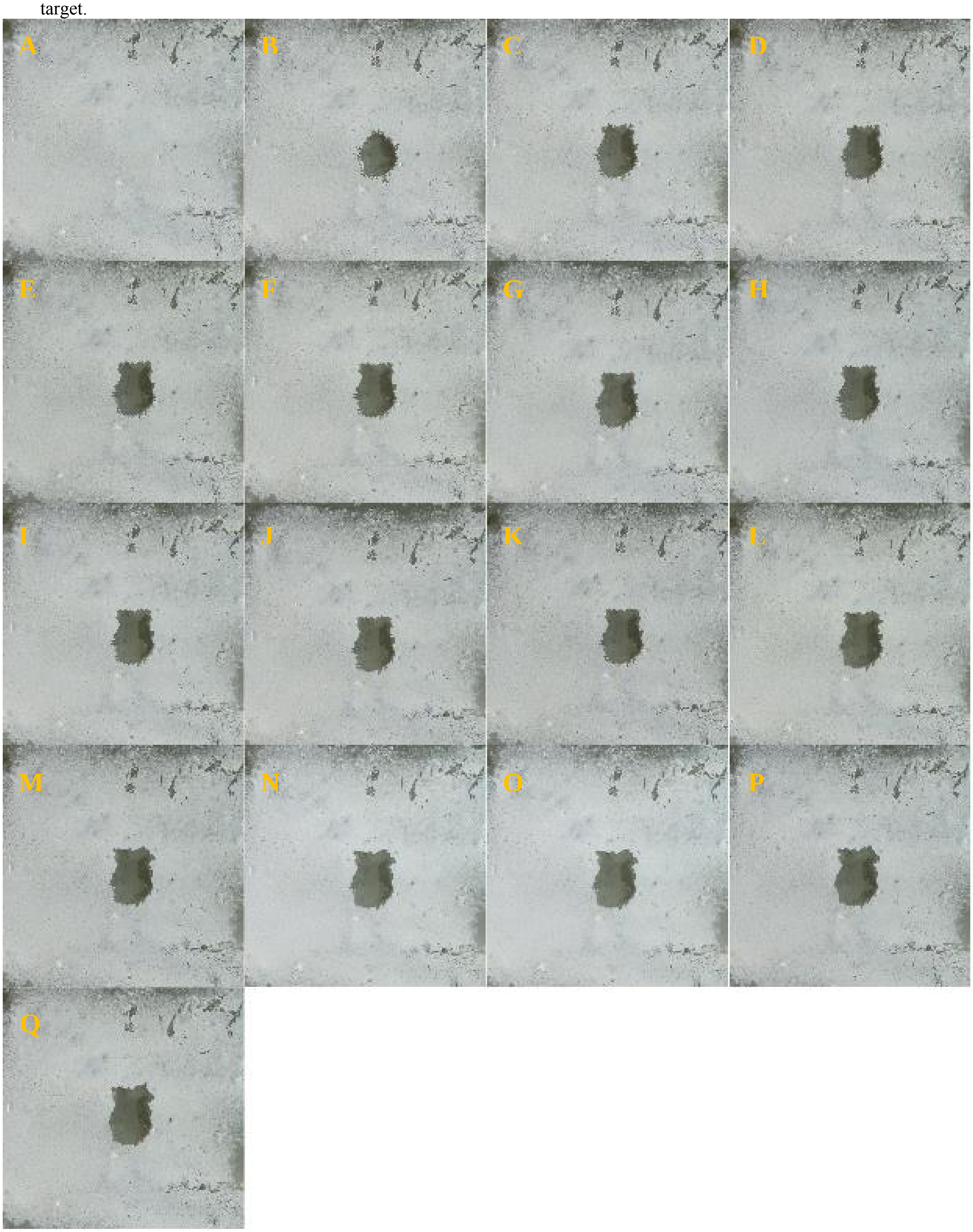

Fig. A12 — DMMP on a PNNL4 coupon. Images of a coupon before application (A) and at 0 (B), 0.5 (C), 1 (D), 1.5 (E), 2 (F), 2.5 (G), 3 (H), 3.5 (I), 4 (J), 4.5 (K), 5 (L), 10 (M), 15 (N), 20 (O), 25 (P), and 30 (Q) min following application of the target.

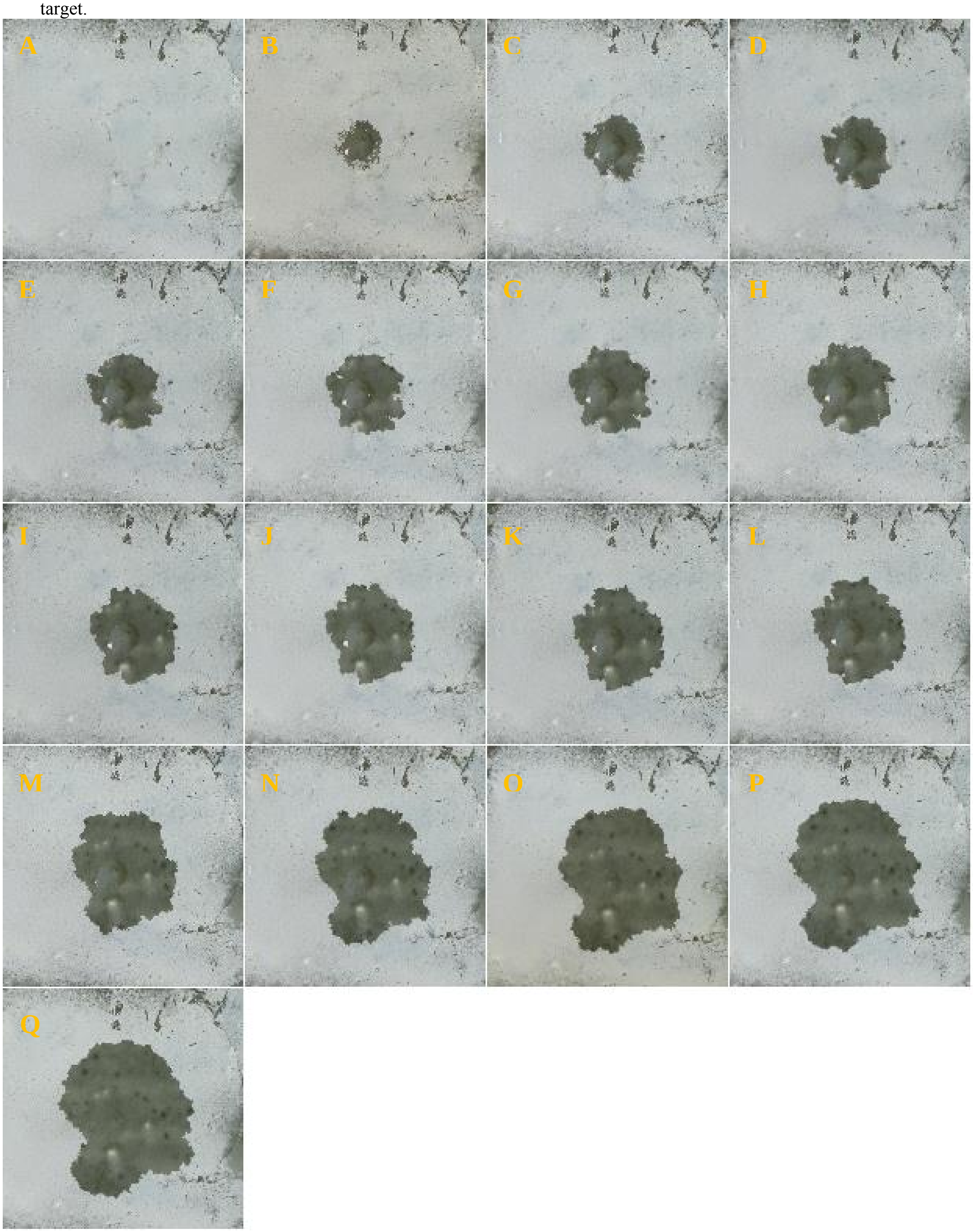

Fig. A13 — DFP on a PNNL5 coupon. Images of a coupon before application (A) and at 0 (B), 0.5 (C), 1 (D), 1.5 (E), 2 (F), 2.5 (G), 3 (H), 3.5 (I), 4 (J), 4.5 (K), 5 (L), 10 (M), 15 (N), 20 (O), 25 (P), and 30 (Q) min following application of the target.

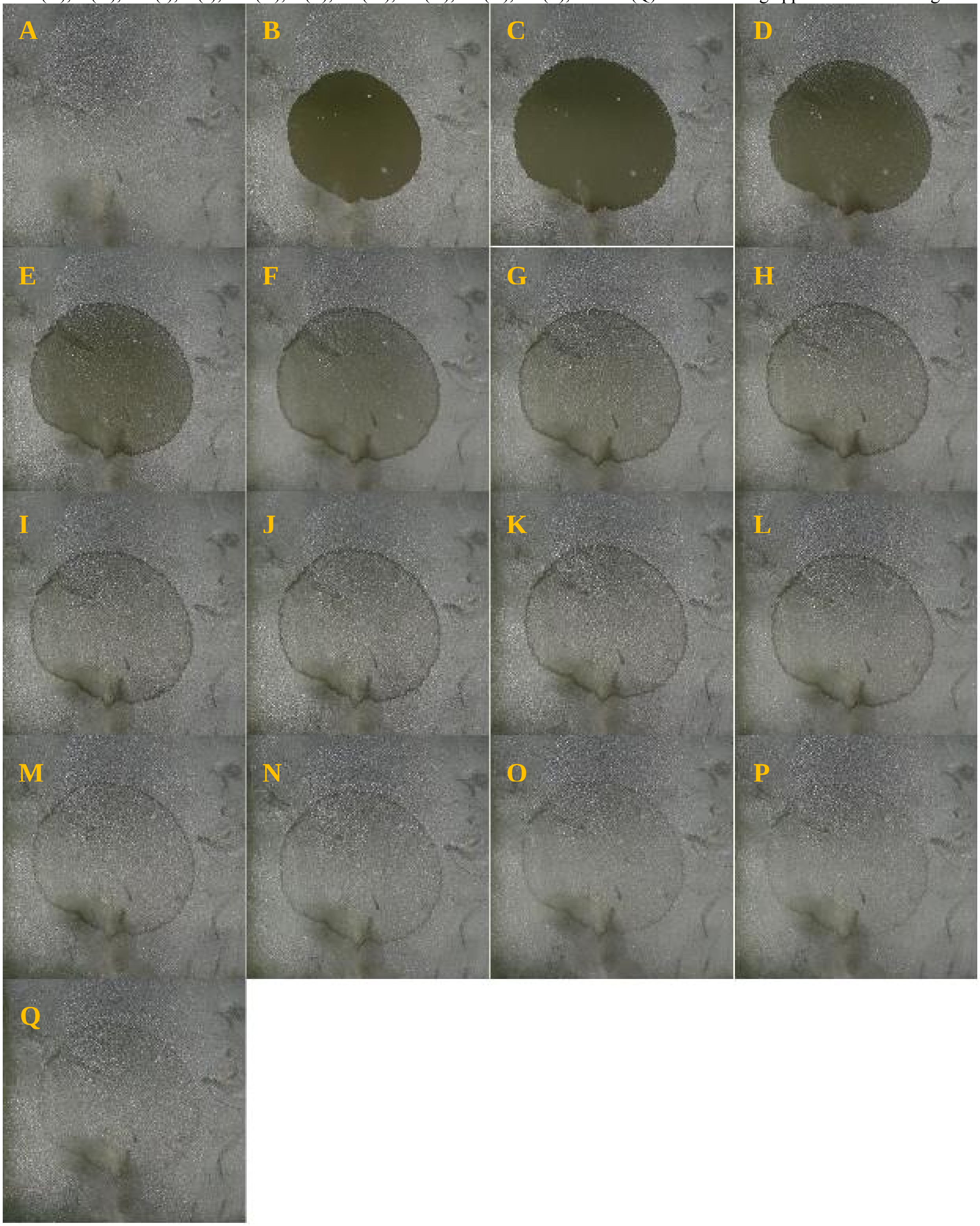

Fig. A14 — MES on a PNNL5 coupon. Images of a coupon before application (A) and at 0 (B), 0.5 (C), 1 (D), 1.5 (E), 2 (F), 2.5 (G), 3 (H), 3.5 (I), 4 (J), 4.5 (K), 5 (L), 10 (M), 15 (N), 20 (O), 25 (P), and 30 (Q) min following application of the target.

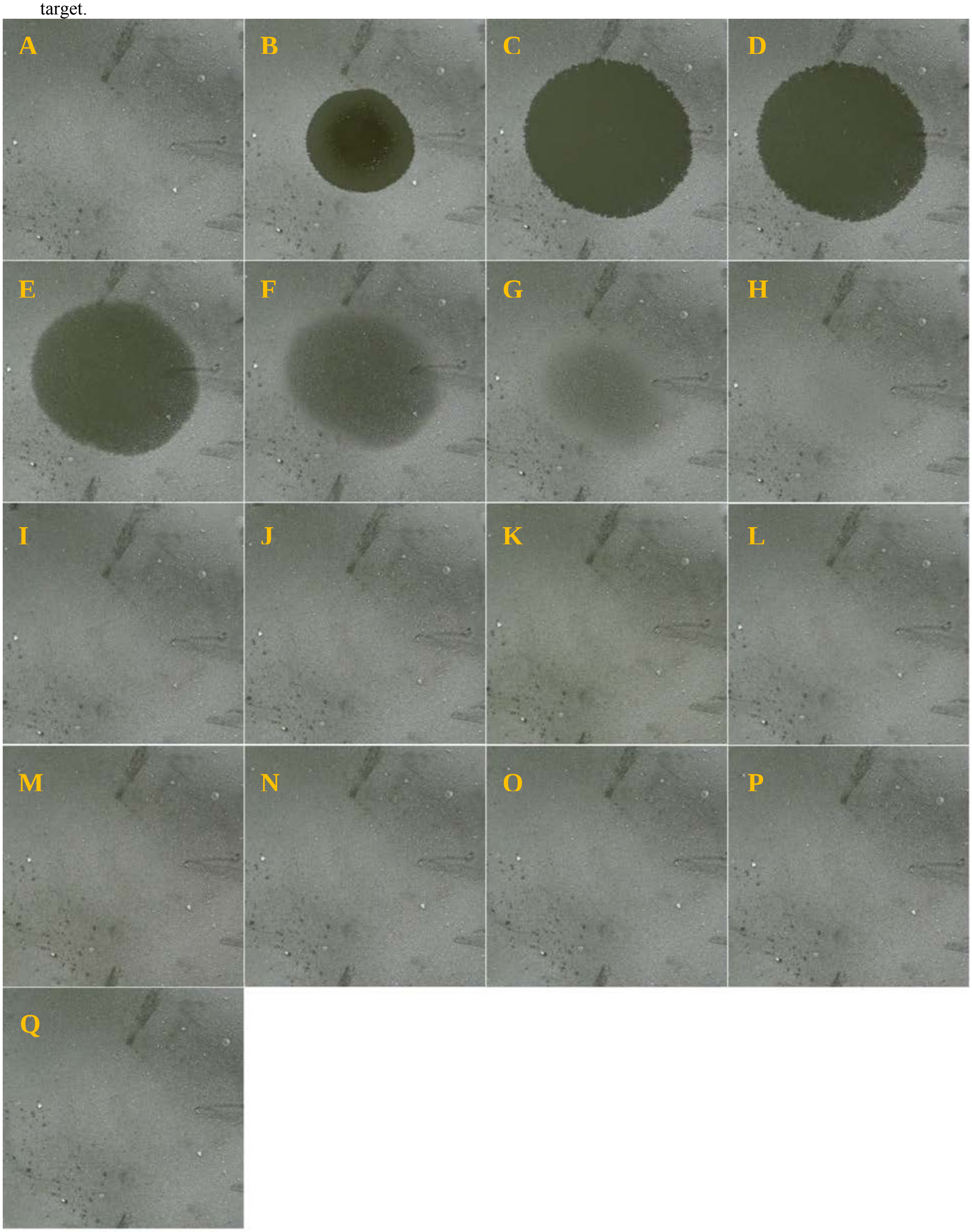

Fig. A15 — DMMP on a PNNL5 coupon. Images of a coupon before application (A) and at 0 (B), 0.5 (C), 1 (D), 1.5 (E), 2 (F), 2.5 (G), 3 (H), 3.5 (I), 4 (J), 4.5 (K), 5 (L), 10 (M), 15 (N), 20 (O), 25 (P), and 30 (Q) min following application of the target.

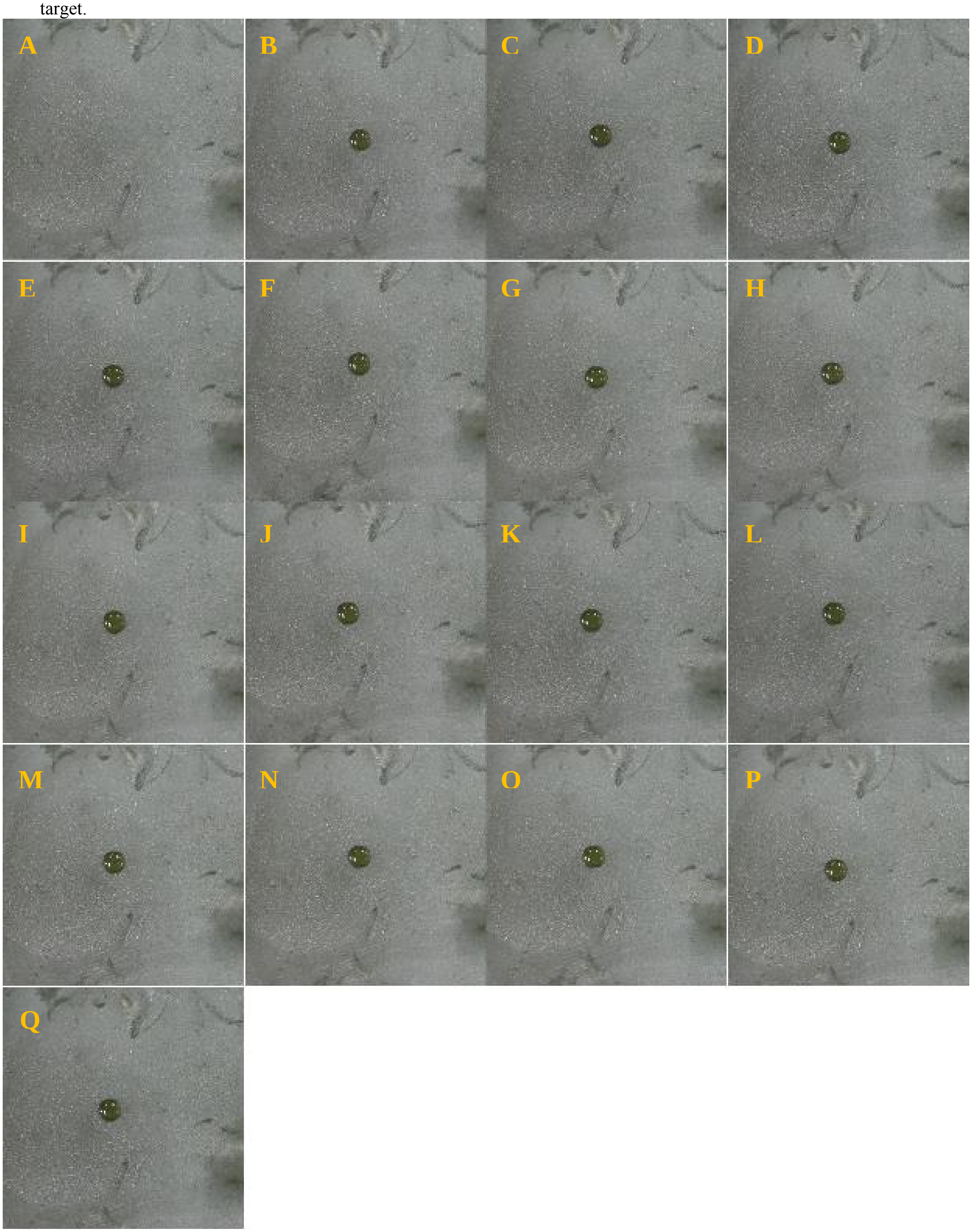

Fig. A16 — DFP on a paint only coupon. Images of a coupon before application (A) and at 0 (B), 0.5 (C), 1 (D), 1.5 (E), 2 (F), 2.5 (G), 3 (H), 3.5 (I), 4 (J), 4.5 (K), 5 (L), 10 (M), 15 (N), 20 (O), 25 (P), and 30 (Q) min following application of the target.

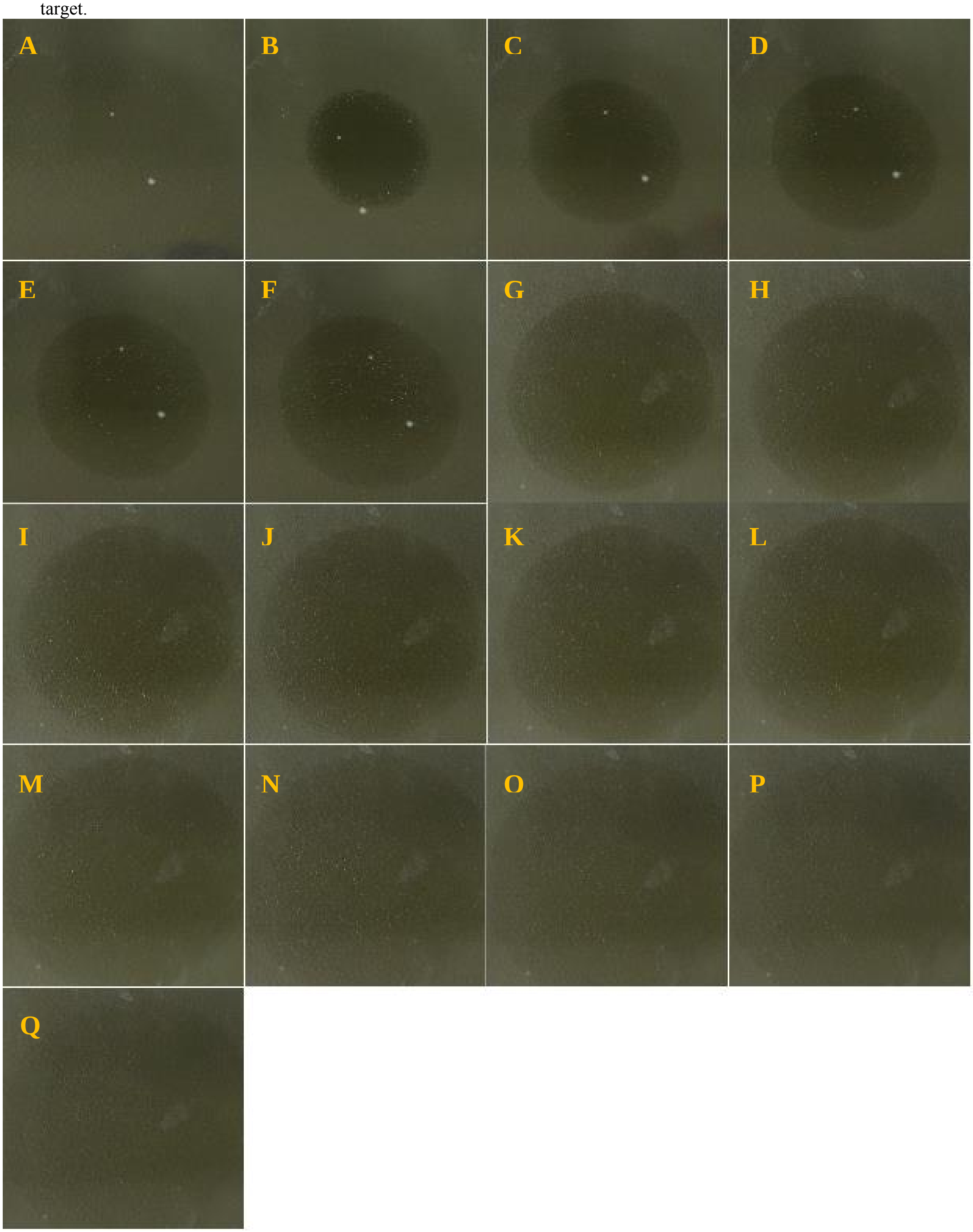

Fig. A17 — MES on a paint only coupon. Images of a coupon before application (A) and at 0 (B), 0.5 (C), 1 (D), 1.5 (E), 2 (F), 2.5 (G), 3 (H), 3.5 (I), 4 (J), 4.5 (K), 5 (L), 10 (M), 15 (N), 20 (O), 25 (P), and 30 (Q) min following application of the target.

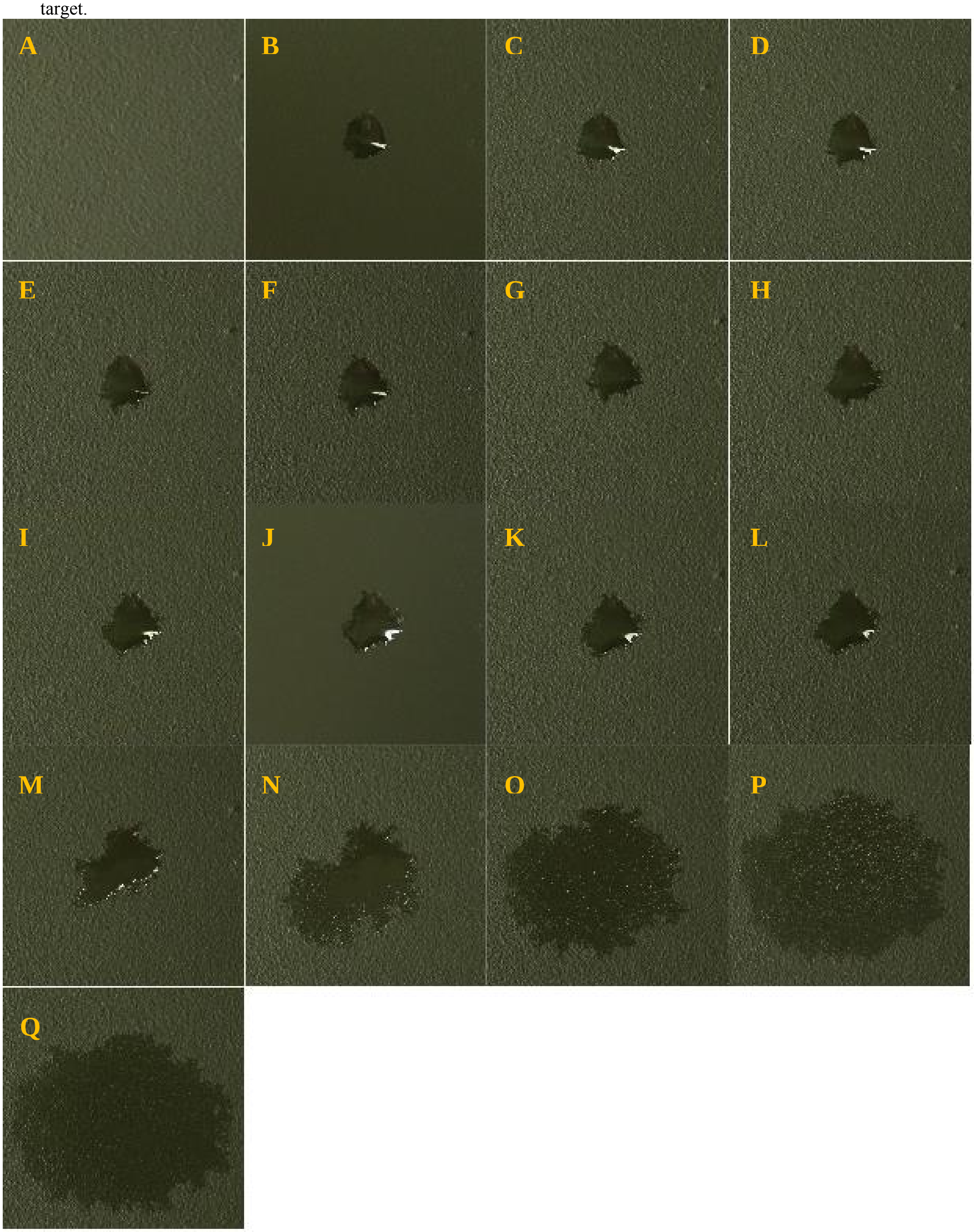

Fig. A18 — DMMP on a paint only coupon. Images of a coupon before application (A) and at 0 (B), 0.5 (C), 1 (D), 1.5 (E), 2 (F), 2.5 (G), 3 (H), 3.5 (I), 4 (J), 4.5 (K), 5 (L), 10 (M), 15 (N), 20 (O), 25 (P), and 30 (Q) min following application of the target.